Biological Psychiatry: CNNI

Archival Report

Individualized Functional Brain System Topologies and Major Depression: Relationships Among Patch Sizes and Clinical Profiles and Behavior

Matthew D. Sacchet, Poorvi Keshava, Shane W. Walsh, Ruby M. Potash, Meiling Li, Hesheng Liu, and Diego A. Pizzagalli

ABSTRACT

BACKGROUND: Neuroimaging studies of major depression have typically been conducted using group-level approaches. However, given interindividual differences in brain systems, there is a need for individualized approaches to brain systems mapping and putative links toward diagnosis, symptoms, and behavior.

METHODS: We used an iterative parcellation approach to map individualized brain systems in 328 participants from a multisite, placebo-controlled clinical trial. We hypothesized that participants with depression would show abnormalities in salience, control, default, and affective systems, which would be associated with higher levels of self-reported anhedonia, anxious arousal, and worse cognitive performance. Within hypothesized brain systems, we compared patch sizes (number of vertices) between depressed and healthy control groups. Within depressed groups, abnormal patches were correlated with hypothesized clinical and behavioral measures.

RESULTS: Significant group differences emerged in hypothesized patches of 1) the lateral salience system (parietal operculum; $t_{326} = -3.11$, $p = .002$) and 2) the control system (left medial posterior prefrontal cortex region; $z = -3.63$, $p < .001$), with significantly smaller patches in these regions in participants with depression than in healthy control participants. Results suggest that participants with depression with significantly smaller patch sizes in the lateral salience system and control system regions experience greater anxious arousal and cognitive deficits.

CONCLUSIONS: The findings imply that neural features mapped at the individual level may relate meaningfully to diagnosis, symptoms, and behavior. There is strong clinical relevance in taking an individualized brain systems approach to mapping neural functional connectivity because these associated region patch sizes may help advance our understanding of neural features linked to psychopathology and foster future patient-specific clinical decision making.

https://doi.org/10.1016/j.bpsc.2024.02.011

Major depressive disorder (MDD) is a debilitating mental health condition that affects millions of individuals globally and is associated with staggering costs (1,2). Despite frameworks prioritizing a push toward system-based and individualized approaches (3–6) to better address the heterogeneity of depression, there remains persistent difficulty in developing personalized treatments (7–9). Relatively few patients with depression reach remission (7–9) and many will experience relapse (10,11).

Given these substantial challenges, there is an urgent need for improved biological models of mental illness that build upon brain mapping approaches that may be able to identify underlying mechanistic processes of psychopathology (12). Spatially distributed and discrete neural regions that display highly correlated activity are referred to as brain systems, or networks, and this correlated activity is thought to reflect neural relationships within the brain (6,13–15). A variety of computational approaches have identified several relevant brain systems at an aggregated group level (16), including the affective, default, frontoparietal, and salience systems, which have been implicated in MDD (17–20). It has been proposed that abnormalities in these systems underlie psychological and behavioral features of psychopathology in MDD (17–20).

However, conclusions drawn from group-level brain system mapping may incorrectly assume that group-level neural functioning can be generalized directly to individuals. Consistent with this conundrum, a recent meta-analysis of 92 group-level neuroimaging studies of depression reported little convergence in findings (21), possibly due to imprecision of group-level quantifications for systems of interest, variability from intersystem blurring/nontarget systems for seed-based analyses, or the selected independent components. Small sample sizes are particularly susceptible to these issues, including biomarker prediction studies (22–28) that have

 ISSN: 2451-9022

typically included fewer than 30 participants (28,29). Given the heterogeneity of individual brain systems, taking a more person-specific approach is critical for improving the use of neuroscientific tools to aid clinical intervention (3).

Therefore, we aimed to apply an individualized brain systems functional brain mapping approach to better account for heterogeneity in neural architecture at the individual level. This approach was based on a previously described iterative optimization method (3–5,30). We aimed to develop a nuanced neuroscientific understanding of depression by identifying connections between person-specific neural functioning and symptom profiles. Such individualized approaches are rapidly gaining traction, with many studies having identified findings that are not observable using group-level approaches (4,5,30). Furthermore, individualized system patches (i.e., sets of proximal cortical vertices that belong to the same brain system) reflect person-specific functional organization and thus do not have a direct equivalent measure in group-level approaches (wherein brain system patches are assumed to be the same across individuals) (16). Here, patches refer to nodes or distinct regions of the brain that exhibit functional homogeneity and highly correlated activity (6,13,14). Patch sizes have substantial biological relevance given that the amount of brain devoted to a given function predicts functional importance or capability (31). For example, larger hippocampi predict memory performance (32), the size of functionally defined visual regions predicts reading skills (33), and auditory association cortex predicts musical ability (34). Additionally, prior studies have provided evidence that patch sizes are related to behavior and mentation. For example, Kong *et al.* recently found that patch sizes were related to behavior (e.g., reading pronunciation and delay discounting) and personality measures (the NEO Personality Inventory) (31).

Preliminary studies (17–19) using aspects of this approach have found that individualized brain systems–based functional connectivity—and notably, not traditional group-level functional connectivity—was linked to dimensional and categorical features of psychosis (30), memory impairments, and electroconvulsive therapy outcomes in individuals with severe depression (35) and dissociative symptoms in trauma-related disorders alongside individual patch size associations (36). Moreover, prior research that has used patch sizes and functional connectivity in conjunction has led to better prediction of measures of interest (e.g., behavioral tasks that probe learning or memory) than connectivity or region size alone, which suggests that patch size may supply unique information (4). Similarly, purported links between neural features and self-report and behavior that have emerged from individualized functional connectivity analyses have outperformed traditional group-level connectivity approaches (35). Collectively, these findings indicate that the relative presence and size of person-specific functional brain regions (individualized brain systems) may provide novel insights into a person-centric brain-based understanding of a highly heterogeneous disorder such as MDD. More importantly, these differences in patch sizes can only be identified using individualized approaches because there is no group equivalent given that group-based approaches use a standardized template atlas for all participants. By definition, this involves prescribing standard patch locations and sizes across participants, thus making it impossible to compare any nuanced differences in the same.

Therefore, we applied a recently developed iterative brain mapping procedure (3) coupled with a patch matching method to understand relationships among individualized patch sizes and diagnosis of MDD, symptom expression, and behavioral measures of inhibitory control by testing 1) for differences in individualized neural patch size between individuals with depression and healthy individuals; 2) putative relationships between path topology and symptom and behavior profiles; 3) geometric features of identified abnormal neural topologies; and finally, 4) quantitative decoding of identified neural regions using NeuroSynth (4,37) for additional interpretive leverage. We tested this approach in regions of interest (ROIs) implicated in MDD (17–20,38) that are core nodes of brain systems, hypothesizing that abnormal patch sizes would be present in the salience (insular and dorsomedial prefrontal cortical and amygdalar regions), control (lateral prefrontal and parietal cortical and hippocampal regions), default (medial prefrontal and parietal cortex), and affective (ventromedial, lateral cortical and striatal regions) areas (17–19,38) and subsequent relationships among identified abnormal specific brain systems regions and processes associated with those systems: anxious arousal (salience) (39), self-reported anhedonia (affective) (40), and cognitive deficits (control) (41), and overall depressive symptoms.

METHODS AND MATERIALS

Participants

From a total of 336 participants, we included 328 participants (66% female, 34% male) ages 18 to 65 years who had completed magnetic resonance imaging (MRI) scans and met criteria for MDD (n = 288) or healthy control participants (n = 40) (for further information on participant demographics, see Participant Information in the Supplement). All participants with MDD in the study were unmedicated at baseline.

Behavioral and Symptom Measures

The Quick Inventory of Depressive Symptomatology-Self Report, Hamilton Depression Rating Scale, Snaith-Hamilton Pleasure Scale, and Mood and Anxiety Symptom Questionnaire were used to assess various symptom dimensions (e.g., anxious arousal, anhedonia, general distress, depression severity), whereas the probabilistic reward task, flanker task, and A-not-B task were used to assess reward learning, response conflict, and working memory, respectively (see Supplemental Methods; for information on data included, see Table S1).

MRI Acquisition and Preprocessing

MRI acquisition and preprocessing were completed using common approaches (for details, see MRI Acquisition and Preprocessing in the Supplement; for information on data included, see Table S2).

Procedures

The current study included preexisting multisite clinical trial data from the EMBARC (establishing moderators and

biosignatures of antidepressant response in clinical care) study (42). Detailed information regarding EMBARC has been published previously (42).

Individualized Brain Systems. An iterative parcellation approach was used (3) to map individualized brain systems. Briefly, functional mapping was initialized using a group-level functional system atlas [Yeo *et al*. (16)], which was then systematically and repeatedly adjusted by incorporating interindividual variability and signal-to-noise ratio distributions per participant to arrive at idiosyncratic person-specific brain maps (4). With each iteration, the influence from group-level information was lessened until the final system map quantitively converged on individualized neural systems mapping (3). For additional information, see Mapping Cortical Individualized Brain Systems in the Supplement. These individually derived cortical brain systems were then separated into patches using a computational neuroimaging algorithmic approach that matched patches to 116 cortical parcellated regions previously labeled in an atlas (4). That is, patches were labeled with converging regions based on overlapping vertices (≥20) and nearest-neighbors approaches based on geodesic distance of neural surfaces. If a patch overlapped with more than one ROI present within the network, then the patch was divided into multiple smaller ROIs. This patch matching and labeling approach enabled group-level analysis of individualized patches. For additional details about this approach, see Li *et al.* (4).

Statistical Approach

Patch Size and Diagnosis. Patch sizes (i.e., number of vertices) within hypothesized brain systems were compared between MDD and healthy control groups. All patches were regressed against variables of noninterest including site, age, and sex, and resulting residuals were subsequently analyzed. This was primarily done to control for effects of these nuisance variables. If significant differences were identified between groups in motion (framewise displacement [FD] or percent signal change across frames), then these measures were also regressed on patch size to account for possible unintended effects of motion. In this case, all patches were regressed against FD. Prior to testing for group differences, normality of distribution was assessed for residualized data. To test for group differences in patch sizes, *t* tests were performed on normally distributed patches (e.g., parietal operculum), and Wilcoxon tests were performed for nonnormally distributed patches (e.g., left medial posterior prefrontal cortex). False discovery rate (FDR) correction was used to account for multiple comparisons within each hypothesized brain system; for example, if a brain system had 5 ROIs, then significant findings within this system were corrected across the 5 *p* values from ROIs within the system (see Figure 1 for an overview of ROIs in brain systems). We focused on systems implicated in MDD: affective, default, frontoparietal, and salience (17–20,38). Several of these may be involved in the symptoms and

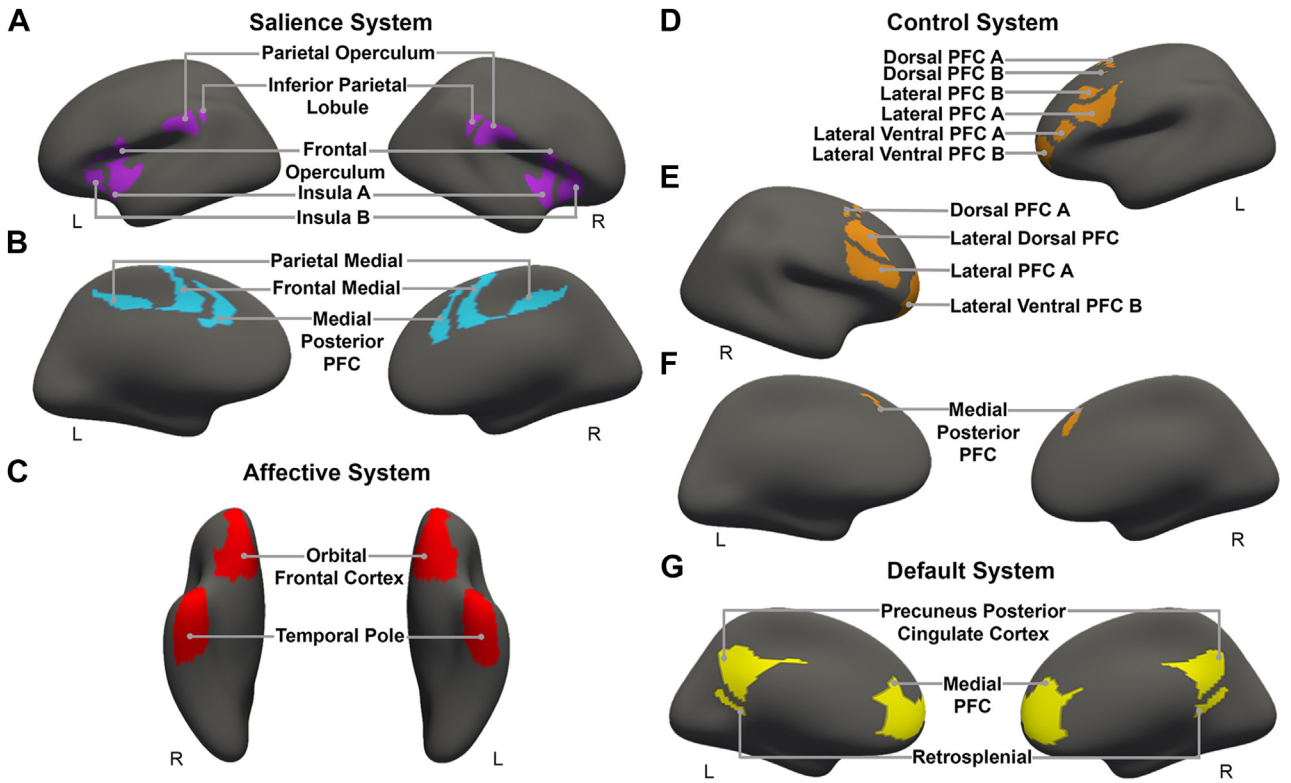

Figure 1. Regions of interest within each brain system: **(A)** lateral salience system; **(B)** medial salience system; **(C)** affective system; **(D–F)** control system [**(D)** left control system, **(E)** right control system, **(F)** medial control system]; and **(G)** default system. Brain regions are color-coded based on each set of false discovery rate–corrected analyses. L, left hemisphere; PFC, prefrontal cortex; R, right hemisphere.

behavior assessed here: anxiety [salience (39)], anhedonia [affective (40)], and cognitive deficits [frontoparietal (41)].

Patch Size and Symptoms and Behavior. Next, we further analyzed patch size significantly differing between the MDD and healthy control groups. Within the MDD group, identified patch size residuals were correlated with hypothesized clinical and behavioral measures to determine relationships among patch size and symptoms and behavior. Prior testing for group differences, normality of distribution was assessed for relevant residualized patch size data as well as behavioral variables. Pearson correlations were used if both variables were normally distributed, and Spearman correlations were used if either or both of the variables tested had a nonnormal distribution. For each brain system region that exhibited group differences, targeted analyses were conducted without correction (see Figure 1). Multiple comparison correction of statistical tests was only applied within behavioral variables that tested the same domain. In this case, multiple comparison correction was only applied to flanker and A-not-B scores.

Coordinate Analysis. If a patch displayed significant differences in size between MDD and healthy control groups, we further tested for differences in its center of mass coordinates following the same steps outlined above for patch sizes. That is, the coordinates were correlated against clinical and behavioral measures using the same steps outlined above for symptoms and behavior, with FDR correction applied.

NeuroSynth. We used the meta-analytic decoding feature of NeuroSynth (37) to identify key terms associated with patches related to MDD. NeuroSynth is a large repository of neural activation coordinates, associated key terms across prior neuroimaging findings, and meta-analytic framework (>14,000 studies, >1300 terms). NeuroSynth enabled a data-driven interpretation of brain regions rather than relying on reverse inference (43).

RESULTS

Movement

There was a significant difference in FD between participants with MDD ($n = 288$) and healthy control participants ($n = 40$) ($z = 3.097$, $p = .002$). Percent signal change between volumes was not significantly different in both groups ($z = 1.376$, $p = .169$). As a result, all patches were regressed against an FD-weighted average (along with other variables of noninterest) before further analyses were conducted.

Relationships Between Patch Size and Diagnosis

Following FDR correction, significant differences between participants with depression and healthy control participants emerged in the parietal operculum region of the lateral salience system ($t_{326} = -3.11$, $p = .002$) and the left hemisphere medial posterior prefrontal cortex region from the control system ($z = -3.63$, $p < .001$) (Figures 1 and 2). For both regions, average patch sizes for participants with depression were smaller than that of control participants (Figure 2; Table 1). To strengthen our findings and control for the putative influence of different surface areas potentially occupied by a given vertex, we also ran an exploratory analysis to test for differences in surface areas between the parietal operculum and left medial posterior prefrontal cortex region. We found that our results remained unchanged and that both regions showed significantly smaller surface areas in participants with MDD than in healthy control participants (see Table S6). This underscores our confidence in the patch size methodology and our results. There were no other significant group differences in patch size of other lateral salience or control system patches. Similarly, we found no significant differences in patch sizes within the hypothesized medial salience, default, and affective systems. All results from patch size analyses between the depressed and control groups are summarized in Table 1.

Relationships Among Patch Size and Symptoms and Behavior in the MDD Sample

Larger MDD parietal operculum patch sizes were significantly correlated with lower anxious arousal ($r = -0.13$, $p = .030$) and lower reward learning ($r = -0.14$, $p = .025$), as assessed with the Mood and Anxiety Symptom Questionnaire and the probabilistic reward task, respectively (Figure 3). The parietal operculum was not significantly correlated with any other hypothesized clinical/behavioral measure (all $|r|$s ≤ 0.12, all ps $\geq .066$).

Larger left hemisphere medial posterior prefrontal cortex patch sizes within participants with MDD were significantly correlated with lower performance on a task probing working memory and reasoning (A-not-B task total correct responses $r = -0.16$, $p = .008$) and higher flanker interference effects on accuracy ($r = 0.12$, $p = .048$) (Figure 3). However, the flanker interference effects on accuracy did not survive FDR correction. This region was not significantly correlated with any other hypothesized clinical/behavioral measures (all $|r|$s ≤ 0.12, all ps $\geq .064$).

Secondary correlations between MDD patch sizes and nonprimary variables of interest (e.g., additional flanker results for on-time trials and Gratton) were consistent with the primary correlational findings, see Figure S1.

Patch Size Geometry: Coordinate Analysis

Coordinate analyses following FDR correction showed that the right hemisphere y coordinate of the parietal operculum was located more anteriorly in participants with depression than in healthy control participants ($z = 2.71$, $p = .007$). No other coordinates of the right or left parietal operculum showed significant group differences. Additionally, no coordinates of the left hemisphere medial posterior prefrontal cortex differed significantly between groups.

The right hemisphere y coordinate of the parietal operculum was significantly correlated with Mood and Anxiety Symptom Questionnaire general distress ($r = 0.15$, $p = .009$). No other clinical or behavioral measure correlations emerged (all $|r|$s ≤ 0.11, ps $\geq .071$).

NeuroSynth

As illustrated in Table S3, results indicated that the parietal operculum region of the lateral salience system was positively

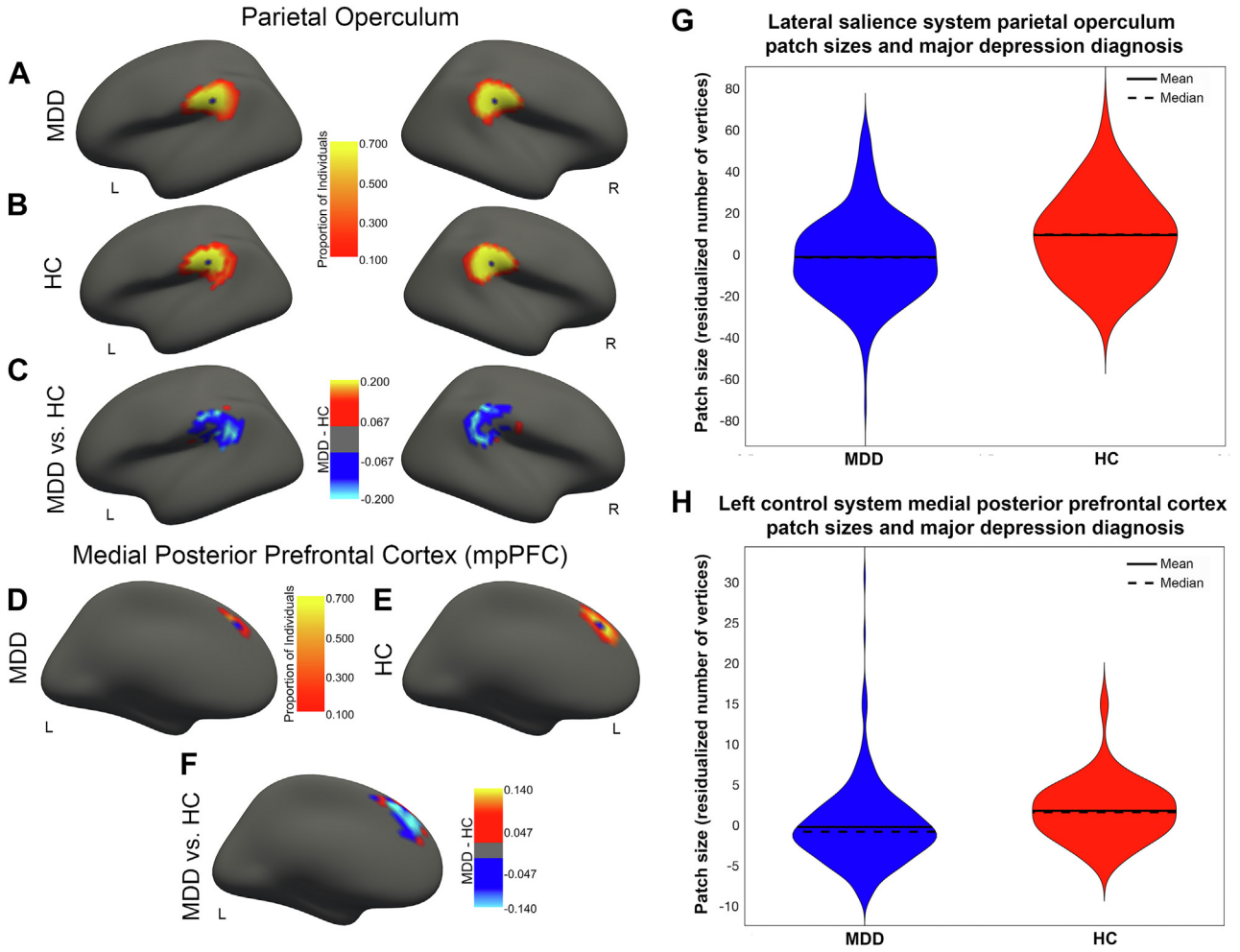

Figure 2. Individualized brain systems patch size differences between major depressive disorder (MDD) and healthy control participant (HC) groups. (Upper) Regions exhibiting group differences included the parietal operculum region of the lateral salience system [**(A)** MDD; **(B)** HC; **(C)** difference between MDD and HC groups] and the left hemisphere (L) medial posterior prefrontal cortex region of the control system [**(D)** MDD; **(E)** HC; **(F)** difference between MDD and HC groups]. **(G)** Patch sizes of the parietal operculum for participants with MDD and HCs. **(H)** Patch sizes of the medial posterior prefrontal cortex for participants with MDD and HCs. R, right hemisphere.

correlated with meta-analytic terms spanning somatic/somatosensory domains (e.g., somatosensory, pain, touch) and negatively correlated with terms related to memory (e.g., autobiographical, memory, episodic). Conversely, the left hemisphere medial posterior prefrontal cortex of the control system was related to meta-analytic terms that spanned cognitive domains including reasoning and decision making (e.g., reasoning, judgment, retention).

DISCUSSION

By applying recently developed computational neuroimaging approaches to map neural functional patches that are individualized to each participant, we were able to link individualized neural architecture to diagnostic, symptom, and behavioral profiles. Analyzing abnormal patch sizes in clinical populations is a unique advantage that is only afforded by individualized approaches. In fact, there is no equivalent group-level approach because group-based approaches use a standardized template atlas for all participants, which involves fitting standardized patch locations and sizes across participants. Therefore, our findings highlight the promise of this approach and provide a foundation for continued implementation of individualized methods to relate neural activity to features of mental illness given their relationship to correlated functional activity (6,13,14). This includes symptoms, behavior, and general functioning for the individual beyond an aggregate group-level brain map.

It is well known that the amount of brain that is devoted to a given function predicts functional importance or capability (31). For example, larger hippocampi predict memory performance (32), the size of functionally defined visual regions predicts reading skills (34), and auditory association cortex predicts musical ability (34). More recent studies have provided additional evidence that patch sizes reflect the boundaries of functional units of the brain. While existing studies are informative, additional research is required to fully understand the

Table 1. Individualized Brain System Patch Sizes by Group: Descriptive Summary of Group Patch Sizes Across Neural Regions for MDD and HC Groups

	MDD		HC			
Region	Mean/Median	SD/IQR	Mean/Median	SD/IQR	*p* Value	Test Statistic
Lateral Salience System						
Insula A[a]	−0.498	18.406	0.025	16.087	.827	0.218
Insula B[a]	−0.368	18.157	0.664	14.104	.465	−0.730
Frontal operculum[a]	−1.355	15.855	−0.652	13.561	.642	0.465
Parietal operculum[b]	−1.284	20.170	9.246	19.494	.002[c]	−3.106
Inferior parietal lobule[a]	−0.415	11.591	−0.946	11.770	.656	−0.446
Medial Salience System						
Medial posterior prefrontal cortex[a]	−1.313	21.911	−1.524	13.966	.426	0.796
Frontal medial[a]	−0.627	18.820	2.206	15.248	.342	−0.949
Parietal medial[b]	−0.266	15.227	1.917	14.126	.392	−0.857
Control System						
L dorsal prefrontal cortex A[b]	0.006	6.880	−0.043	5.904	.966	0.043
L dorsal prefrontal cortex B[a]	−0.430	11.033	−1.909	8.857	.909	0.115
L lateral prefrontal cortex B[a]	−0.525	9.927	−0.575	7.542	.671	−0.424
L medial posterior prefrontal cortex B[a]	−0.850	4.904	1.589	4.458	<.001[d]	−3.634
R medial posterior prefrontal cortex B[a]	−1.104	7.837	0.998	7.021	.053	−1.937
R lateral prefrontal cortex A[a]	−0.150	15.907	2.384	10.915	.691	−0.398
L lateral ventral prefrontal cortex A[a]	−0.119	6.277	0.545	6.908	.244	−1.165
R lateral dorsal prefrontal cortex B[b]	−0.153	10.416	1.099	9.254	.471	−0.721
R dorsal prefrontal cortex A[b]	−0.073	8.287	0.524	8.244	.670	−0.427
L lateral prefrontal cortex A[b]	−0.102	9.035	0.737	7.021	.573	−0.564
L lateral ventral prefrontal cortex B[b]	−0.282	10.235	2.032	8.109	.171	−1.371
R lateral ventral prefrontal cortex B[a]	−0.604	12.886	0.244	15.059	.752	−0.316
Default System						
Precuneus posterior cingulate cortex[b]	0.127	13.137	−0.915	11.184	.633	0.478
Retrosplenial[b]	0.366	12.480	−2.636	13.252	.158	1.415
Medial prefrontal cortex[b]	−0.188	22.866	1.354	20.477	.686	−0.405
Affective System						
Orbital frontal cortex [b]	−0.067	31.361	0.486	24.949	.915	−0.107
Temporal pole[b]	1.058	39.979	−7.621	35.660	.194	1.303

Data are residuals. A and B refer to designations used in the Yeo *et al*. atlas (16). Within this atlas some systems, such as the control system and the ventral attention system (salience system), are further split into A and B systems. For instance, in this context, "L dorsal prefrontal cortex B" indicates that the ROI left dorsal prefrontal cortex lies in the control B system; similarly, "insula A" indicates that this ROI lies in the ventral attention A system.

HC, healthy control participant; L, left hemisphere; MDD, major depressive disorder; R, right hemisphere.

[a]Data were nonnormally distributed, and Wilcoxon rank-sum tests were used for statistical assessment with medians and IQRs reported. Statistical significance indicated following false discovery rate correction:

[b]Data were normally distributed, and *t* tests were used for statistical assessment, with means and SDs reported.

[c]$p < .01$.

[d]$p < .001$.

biology of patches and their pathophysiology in mental illness, and we hope this investigation provides evidence to support the use of individualized approaches.

Following FDR correction, hypothesized neural patches of 1) the lateral salience system (parietal operculum) and 2) the control system (left medial posterior prefrontal cortex region) were significantly smaller in participants with depression than in healthy control participants. NeuroSynth findings suggested that the former was associated with somatic and somatosensory domains and the latter with cognition, reasoning, and decision making. However, no differences were identified in the affective and default systems, which contrasts with prior findings of group-level clinical differences in such regions (24,27). These differences may be accounted for by the methods used to assess differences given that we probed the functional topography of individualized regions. Future work could evaluate whether individual differences in affective and default system patches differ from more prototypical group-averaged affective and default system activation.

Consistent with the group comparison (MDD < healthy control), smaller patch sizes of the parietal operculum region were further associated with higher self-reported levels of anxious arousal. However, contrary to expectation, larger patch sizes of the parietal operculum were also associated with reduced reward learning (i.e., reduced ability to modulate behavior as a function of rewards). Furthermore, larger patch sizes in the prefrontal cortex region were associated with

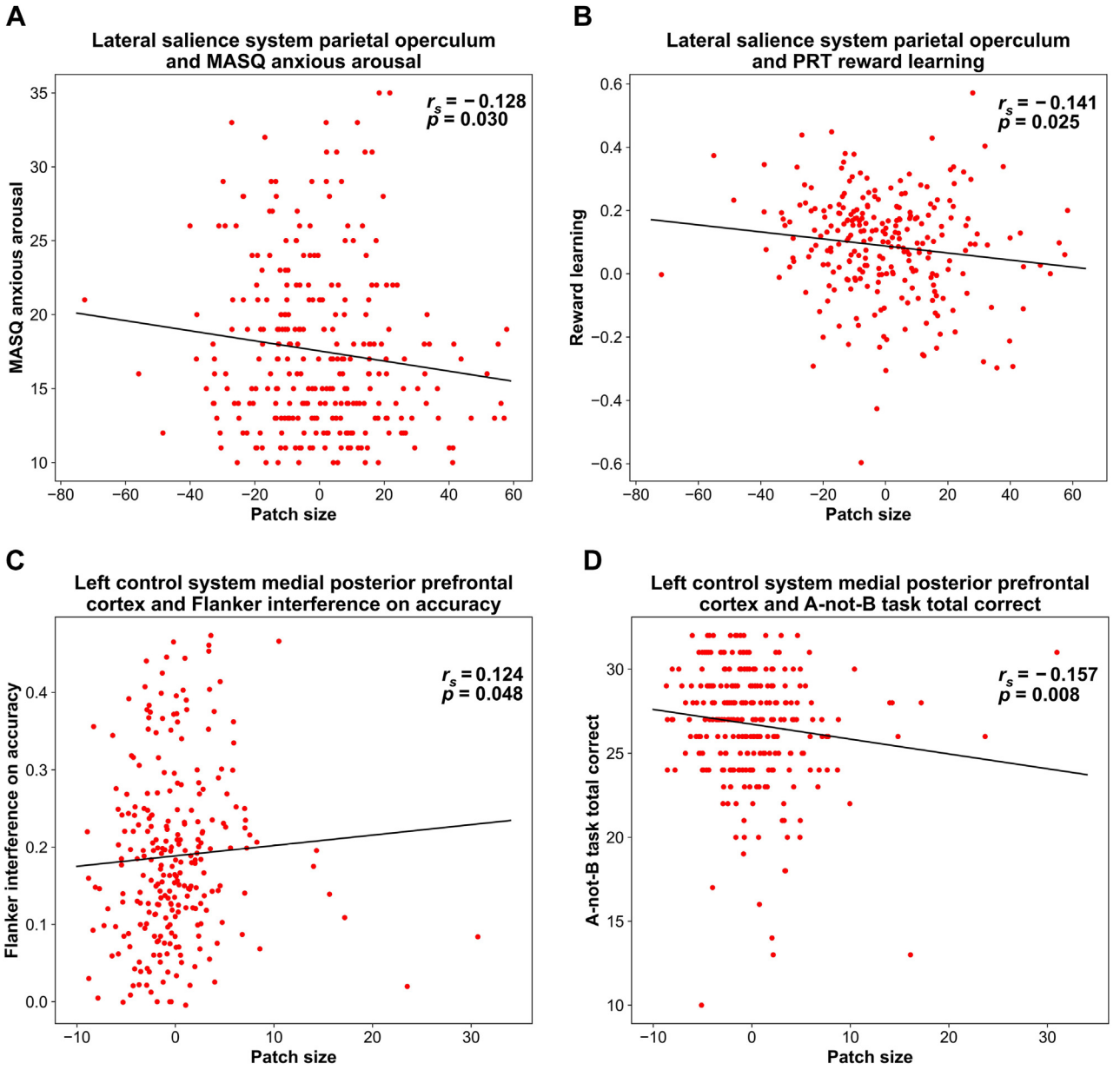

Figure 3. Correlations between brain system patches and self-reported symptoms and behavioral task performance. **(A, B)** Spearman correlations (r_s) between lateral salience system parietal operculum patch size (residualized number of vertices) and clinical and behavioral measures of **(A)** Mood and Anxiety Symptom Questionnaire (MASQ) anxious arousal and **(B)** probabilistic reward task (PRT) reward learning. **(C, D)** Correlations between control system left medial posterior prefrontal cortex patch size and behavioral measures of **(C)** Flanker interference on accuracy and **(D)** A-not-B task total correct.

reduced working memory and reasoning performance and lower cognitive control as measured by the accuracy scores of the flanker and A-not-B task. While this may seem counterintuitive, it is consistent with previous findings. Prior literature has yielded a pattern that suggests that individuals with depression often perform better on cognitive tasks that require accuracy (44). For example, individuals with depression show slower but more accurate performance on flanker and Stroop tasks (44,45). More critically, our previously published paper on an early subset of the EMBARC study reported that the performance of individuals with depression was characterized by slower reaction time but higher accuracy on the flanker task than healthy control individuals (44). One explanation for this finding has been that depressed groups may be engaging in slower, more deliberate information processing that could protect them from forming inaccurate response biases during cognitive tasks (46). This may explain why smaller patch sizes, which were more characteristic of participants with depression, showed an association with improved flanker and A-not-B task performance, but only in relation to measures of accuracy. However, these findings could also merely reflect the vast heterogeneity in depressive disorders. Various studies

have found inconsistent findings related to cognitive impairment, including discrepancies in severity, the cognitive domains affected, and the directionality of cognitive impairments (47,48).

Collectively, these results relate person-specific brain mapping to several levels of analysis that promise to advance our understanding of heterogeneous mental illnesses (8,9,49–52) and further emphasize the importance of salience- (53) and cognition-related (24) neural functioning in depression. Interestingly, the parietal operculum is one of the only regions found to display higher activation in individuals with MDD during reward anticipation but not in reward outcomes (54). The parietal operculum has also been implicated in positive memory recollection among healthy individuals without depression (55). Thus, individual differences appear to highlight the possible impact of this neural area in depression. In the prefrontal cortex, anatomical analyses have pointed to smaller total volume in medial orbital prefrontal cortex regions for people with geriatric depression (56). While in a different neural area, the findings highlighted in our study complement prior work by identifying similar smaller patches. Finally, our assessment of cortical geometry (i.e., coordinate analysis) indicated that the parietal operculum was located more anteriorly in participants with MDD, and this pattern was significantly associated with general distress. This statistically significant finding provides evidence for the significance of displacement of patches/ROIs in psychopathology. Future person-specific investigations could be useful for identifying the nuanced role of such displacement in clinical presentations of MDD. Taken together, our results indicate that brain mapping at the individual level is related to diagnosis (e.g., patch size of the lateral salience and control systems), symptoms (e.g., anxious arousal and general distress), and behavior (e.g., reward learning and working memory).

NeuroSynth findings produced useful contextualization of the potential meaning for neural regions that differentiated participants with depression from healthy control participants (Table S3). We assessed the highest positive and negative correlating terms for the lateral parietal operculum and left medial posterior prefrontal cortex. Findings linked patch vertices in the lateral salience parietal operculum with sensory, pain, and tactile terms and negatively associated with memory related terms, which may imply that individuals with depression experience functional problems in such areas and potentially experience such problems due to the smaller topological neural areas associated with these functions. While it is difficult to parse causality, these relationships provide insight into differences between healthy and depressed samples and directions for future research.

In sum, individualized brain systems approaches (3–5,30) advance our understanding of the brain and psychopathology and the development of new hypotheses for future research and may inform patient-specific clinical decisions.

Limitations and Future Directions

Due to the cross-sectional nature of the neuroimaging component in the initial study, it was not possible to assess the causality of the brain regions implicated in MDD. Future studies could utilize an individualized brain systems approach in a longitudinal neuroimaging study of depression to understand causal relationships of these regions in participants with depression. A future longitudinal study could also examine whether these differences in patch sizes represent a trait vulnerability or a state-dependent vulnerability to depression. Additionally, the current study only focused on the implications of cortical regions in individuals with MDD. Future studies should incorporate the cortico-subcortical circuits in similar analyses, which may allow for further insights into individualized functional networks and their role in depression. While the individualized approach overcomes the shortcomings of group-based neuroimaging approaches by accounting for individualized differences in brain mapping, our significant findings were relatively few compared to well-established group-based systems associated with depression (17,19). However, because the patch size metric is not directly comparable to conventional functional connectivity approaches, it is not surprising that our analysis did not replicate the same pattern of results as conventional approaches. Relatedly, another limitation of the current study is that we did not run a traditional functional connectivity analysis to compare results and potentially identify unique contributions of the patch size methodology. However, it is not obvious how to directly relate a measure like patch size, which is a single measure for a given region, to functional connectivity, which conventionally requires the assessment of time courses of activity between 2 regions. Additionally, while it was beyond the scope of our study to integrate treatment outcome data, future studies may benefit from predicting treatment outcomes based on patch sizes derived from individualized approaches. Future studies may also benefit from probing individualized functional organizations on the basis of different variables including but not limited to sex and/or age to identify unique neural differences related to these domains.

ACKNOWLEDGMENTS AND DISCLOSURES

MDS and the Meditation Research Group are supported by the National Institute of Mental Health (Grant No. 1R01MH125850-01A1), Dimension Giving Fund, Ad Astra Chandaria Foundation, Phyllis and Jerome Lyle Rappaport Foundation, Brain and Behavior Research Foundation (Grant No. 28972), Bial Foundation (Grant No. 099/2020), Emergence Benefactors, The Ride for Mental Health, Gatto Foundation, Center for Depression, Anxiety, and Stress Research at McLean Hospital, and individual donors. DAP was partially supported by the National Institute of Mental Health (Grant Nos. R37 MH068376 and P50 MH119467).

The data used in this article were obtained from the EMBARC (Establishing Moderators and Biosignatures of Antidepressant Response in Clinical Care) study (https://clinicaltrials.gov/ct2/show/NCT01407094), which is currently accessible through the National Institute of Mental Health Data Archive (42).

Over the past 3 years, DAP has received consulting fees from Albright Stonebridge Group, Boehringer Ingelheim, Compass Pathways, Engrail Therapeutics, Neumora Therapeutics (formerly BlackThorn Therapeutics), Neurocrine Biosciences, Neuroscience Software, Otsuka, Sunovion, and Takeda; honoraria from the Psychonomic Society and the American Psychological Association (for editorial work) and from Alkermes; research funding from the Brain and Behavior Research Foundation, the Dana Foundation, Millennium Pharmaceuticals, the National Institute of Mental Health, and Wellcome Leap; and stock options from Compass Pathways, Engrail Therapeutics, Neumora Therapeutics, and Neuroscience Software. No funding from these entities was used to support the current work, and all views expressed are solely those of the authors. All other authors report no biomedical financial interests or potential conflicts of interest.

ARTICLE INFORMATION

From the Meditation Research Program, Department of Psychiatry, Massachusetts General Hospital, Boston, Massachusetts (MDS, PK, RMP); Department of Psychiatry, Harvard Medical School, Boston, Massachusetts (MDS, PK, DAP); Center for Depression, Anxiety and Stress Research, McLean Hospital, Belmont, Massachusetts (SWW, DAP); Athinoula A. Martinos Center for Biomedical Imaging, Department of Radiology, Massachusetts General Hospital, Charlestown, Massachusetts (ML, HL); Department of Neuroscience, Medical University of South Carolina, Charleston, South Carolina (HL); and McLean Imaging Center, McLean Hospital, Belmont, Massachusetts (DAP).

Address correspondence to Matthew D. Sacchet, Ph.D., at sacchetadmin@mgh.harvard.edu.

Received May 9, 2023; revised Feb 10, 2024; accepted Feb 19, 2024.

Supplementary material cited in this article is available online at https://doi.org/10.1016/j.bpsc.2024.02.011.

REFERENCES

1. Greenberg PE, Fournier AA, Sisitsky T, Pike CT, Kessler RC (2015): The economic burden of adults with major depressive disorder in the United States (2005 and 2010). J Clin Psychiatry 76:155–162.
2. Myers LL, Wodarski JS (2014): Using the substance abuse and mental health services administration (SAMHSA) evidence-based practice kits in social work education. Res Soc Work Pract 24:705–714.
3. Wang D, Buckner RL, Fox MD, Holt DJ, Holmes AJ, Stoecklein S, *et al.* (2015): Parcellating cortical functional networks in individuals. Nat Neurosci 18:1853–1860.
4. Li M, Wang D, Ren J, Langs G, Stoecklein S, Brennan BP, *et al.* (2019): Performing group-level functional image analyses based on homologous functional regions mapped in individuals. PLoS Biol 17: e2007032.
5. Brennan BP, Wang D, Li M, Perriello C, Ren J, Elias JA, *et al.* (2019): Use of an individual-level approach to identify cortical connectivity biomarkers in obsessive–compulsive disorder. Biol Psychiatry Cogn Neurosci Neuroimaging 4:27–38.
6. Gordon EM, Laumann TO, Adeyemo B, Gilmore AW, Nelson SM, Dosenbach NUF, Petersen SE (2017): Individual-specific features of brain systems identified with resting state functional correlations. Neuroimage 146:918–939.
7. Wittchen HU, Carter RM, Pfister H, Montgomery SA, Kessler RC (2000): Disabilities and quality of life in pure and comorbid generalized anxiety disorder and major depression in a national survey. Int Clin Psychopharmacol 15:319–328.
8. Westen D, Morrison K (2001): A multidimensional meta-analysis of treatments for depression, panic, and generalized anxiety disorder: An empirical examination of the status of empirically supported therapies. J Consult Clin Psychol 69:875–899.
9. Saveanu R, Etkin A, Duchemin AM, Goldstein-Piekarski A, Gyurak A, Debattista C, *et al.* (2015): The International Study to Predict Optimized Treatment in Depression (iSPOT-D): Outcomes from the acute phase of antidepressant treatment. J Psychiatr Res 61:1–12.
10. Kessler RC, Wang PS (2010): The epidemiology of depression. In: Gotlib IH and Hammen CL, editors. Handbook of depression, 2nd ed. New York: Guilford Press, 5–22.
11. Boland RJ, Keller MB (2010): Course and outcome of depression. In: Gotlib IH and Hammen CL, editors. Handbook of depression, 2nd ed. New York: Guilford Press, 23–43.
12. Huys QJM, Maia TV, Frank MJ (2016): Computational psychiatry as a bridge from neuroscience to clinical applications. Nat Neurosci 19:404–413.
13. Biswal B, Yetkin FZ, Haughton VM, Hyde JS (1995): Functional connectivity in the motor cortex of resting human brain using echo-planar MRI. Magn Reson Med 34:537–541.
14. Zhang D, Raichle ME (2010): Disease and the brain's dark energy. Nat Rev Neurol 6:15–28.
15. Dosenbach NUF, Fair DA, Miezin FM, Cohen AL, Wenger KK, Dosenbach RAT, *et al.* (2007): Distinct brain networks for adaptive and stable task control in humans. Proc Natl Acad Sci U S A 104:11073–11078.
16. Yeo BT, Krienen FM, Sepulcre J, Sabuncu MR, Lashkari D, Hollinshead M, *et al.* (2011): The organization of the human cerebral cortex estimated by intrinsic functional connectivity. J Neurophysiol 106:1125–1165.
17. Kaiser RH, Andrews-Hanna JR, Wager TD, Pizzagalli DA (2015): Large-scale network dysfunction in major depressive disorder: A meta-analysis of resting-state functional connectivity. JAMA Psychiatry 72:603–611.
18. Hamilton JP, Farmer M, Fogelman P, Gotlib IH (2015): Depressive rumination, the default-mode network, and the dark matter of clinical neuroscience. Biol Psychiatry 78:224–230.
19. Mulders PC, van Eijndhoven PF, Schene AH, Beckmann CF, Tendolkar I (2015): Resting-state functional connectivity in major depressive disorder: A review. Neurosci Biobehav Rev 56:330–344.
20. Sylvester CM, Corbetta M, Raichle ME, Rodebaugh TL, Schlaggar BL, Sheline YI, *et al.* (2012): Functional network dysfunction in anxiety and anxiety disorders. Trends Neurosci 35:527–535.
21. Gray JP, Müller VI, Eickhoff SB, Fox PT (2020): Multimodal abnormalities of brain structure and function in major depressive disorder: A meta-analysis of neuroimaging studies. Am J Psychiatry 177: 422–434.
22. Alexopoulos GS, Hoptman MJ, Kanellopoulos D, Murphy CF, Lim KO, Gunning FM (2012): Functional connectivity in the cognitive control network and the default mode network in late-life depression. J Affect Disord 139:56–65.
23. Webb CA, Trivedi MH, Cohen ZD, Dillon DG, Fournier JC, Goer F, *et al.* (2019): Personalized prediction of antidepressant v. placebo response: Evidence from the EMBARC study. Psychol Med 49:1118–1127.
24. Etkin A, Patenaude B, Song YJC, Usherwood T, Rekshan W, Schatzberg AF, *et al.* (2015): A cognitive–emotional biomarker for predicting remission with antidepressant medications: A report from the iSPOT-D trial. Neuropsychopharmacology 40:1332–1342.
25. Crowther A, Smoski MJ, Minkel J, Moore T, Gibbs D, Petty C, *et al.* (2015): Resting-state connectivity predictors of response to psychotherapy in major depressive disorder. Neuropsychopharmacology 40:1659–1673.
26. Walsh E, Carl H, Eisenlohr-Moul T, Minkel J, Crowther A, Moore T, *et al.* (2017): Attenuation of frontostriatal connectivity during reward processing predicts response to psychotherapy in major depressive disorder. Neuropsychopharmacology 42:831–843.
27. Williams LM, Korgaonkar MS, Song YC, Paton R, Eagles S, Goldstein-Piekarski A, *et al.* (2015): Amygdala reactivity to emotional faces in the prediction of general and medication-specific responses to antidepressant treatment in the randomized iSPOT-D trial. Neuropsychopharmacology 40:2398–2408.
28. Pringle A, McCabe C, Cowen PJ, Harmer CJ (2013): Antidepressant treatment and emotional processing: Can we dissociate the roles of serotonin and noradrenaline? J Psychopharmacol 27:719–731.
29. Dichter GS, Gibbs D, Smoski MJ (2015): A systematic review of relations between resting-state functional-MRI and treatment response in major depressive disorder. J Affect Disord 172:8–17.
30. Wang D, Li M, Wang M, Schoeppe F, Ren J, Chen H, *et al.* (2020): Individual-specific functional connectivity markers track dimensional and categorical features of psychotic illness. Mol Psychiatry 25:2119–2129.
31. Kong R, Li J, Orban C, Sabuncu MR, Liu H, Schaefer A, *et al.* (2019): Spatial topography of individual-specific cortical networks predicts human cognition, personality, and emotion. Cereb Cortex 29:2533–2551.
32. Erickson KI, Voss MW, Prakash RS, Basak C, Szabo A, Chaddock L, *et al.* (2011): Exercise training increases size of hippocampus and improves memory. Proc Natl Acad Sci U S A 108:3017–3022.
33. Dehaene S, Pegado F, Braga LW, Ventura P, Nunes Filho G, Jobert A, *et al.* (2010): How learning to read changes the cortical networks for vision and language. Science 330:1359–1364.
34. Schlaug G, Jäncke L, Huang Y, Steinmetz H (1995): In vivo evidence of structural brain asymmetry in musicians. Science 267:699–701.
35. Wang D, Tian Y, Li M, Dahmani L, Wei Q, Bai T, *et al.* (2020): Functional connectivity underpinnings of electroconvulsive therapy-induced

memory impairments in patients with depression. Neuropsychopharmacology 45:1579–1587.
36. Lebois LAM, Li M, Baker JT, Wolff JD, Wang D, Lambros AM, *et al.* (2021): Large-scale functional brain network architecture changes associated with trauma-related dissociation. Am J Psychiatry 178:165–173.
37. Yarkoni T, Poldrack RA, Nichols TE, Van Essen DC, Wager TD (2011): Large-scale automated synthesis of human functional neuroimaging data. Nat Methods 8:665–670.
38. Menon V (2011): Large-scale brain networks and psychopathology: A unifying triple network model. Trends Cogn Sci 15:483–506.
39. Downar J, Crawley AP, Mikulis DJ, Davis KD (2000): A multimodal cortical network for the detection of changes in the sensory environment. Nat Neurosci 3:277–283.
40. Rolls ET (2019): The orbitofrontal cortex and emotion in health and disease, including depression. Neuropsychologia 128:14–43.
41. Vincent JL, Kahn I, Snyder AZ, Raichle ME, Buckner RL (2008): Evidence for a frontoparietal control system revealed by intrinsic functional connectivity. J Neurophysiol 100:3328–3342.
42. Trivedi MH, McGrath PJ, Fava M, Parsey RV, Kurian BT, Phillips ML, *et al.* (2016): Establishing moderators and biosignatures of antidepressant response in clinical care (EMBARC): Rationale and design. J Psychiatr Res 78:11–23.
43. Poldrack RA (2011): Inferring mental states from neuroimaging data: From reverse inference to large-scale decoding. Neuron 72:692–697.
44. Dillon DG, Wiecki T, Pechtel P, Webb C, Goer F, Murray L, *et al.* (2015): A computational analysis of flanker interference in depression. Psychol Med 45:2333–2344.
45. Dubal S, Pierson A, Jouvent R (2000): Focused attention in anhedonia: A P3 study. Psychophysiology 37:711–714.
46. Andrews PW, Thomson JA Jr (2009): The bright side of being blue: Depression as an adaptation for analyzing complex problems. Psychol Rev 116:620–654.
47. Hasselbalch BJ, Knorr U, Kessing LV (2011): Cognitive impairment in the remitted state of unipolar depressive disorder: A systematic review. J Affect Disord 134:20–31.
48. Quinn CR, Harris A, Kemp AH (2012): The impact of depression heterogeneity on inhibitory control. Aust N Z J Psychiatry 46:374–383.
49. Galatzer-Levy IR, Bryant RA (2013): 636,120 ways to have posttraumatic stress disorder. Perspect Psychol Sci 8:651–662.
50. Cicchetti D, Dawson G (2002): Multiple levels of analysis. Editorial. Dev Psychopathol 14:417–420.
51. Insel TR (2014): The NIMH Research Domain Criteria (RDoC) Project: Precision medicine for psychiatry. Am J Psychiatry 171:395–397.
52. Insel T, Cuthbert B, Garvey M, Heinssen R, Pine DS, Quinn K, *et al.* (2010): Research domain criteria (RDoC): Toward a new classification framework for research on mental disorders. Am J Psychiatry 167:748–751.
53. Manoliu A, Meng C, Brandl F, Doll A, Tahmasian M, Scherr M, *et al.* (2013): Insular dysfunction within the salience network is associated with severity of symptoms and aberrant inter-network connectivity in major depressive disorder. Front Hum Neurosci 7:930.
54. Smoski MJ, Felder J, Bizzell J, Green SR, Ernst M, Lynch TR, Dichter GS (2009): fMRI of alterations in reward selection, anticipation, and feedback in major depressive disorder. J Affect Disord 118:69–78.
55. Isato A, Yokokawa K, Higuchi M, Suhara T, Yamada M (2022): Resting-state functional connectivity relates to interindividual variations in positive memory. Behav Brain Res 419:113663.
56. Lai T-J, Payne ME, Byrum CE, Steffens DC, Krishnan KRR (2000): Reduction of orbital frontal cortex volume in geriatric depression. Biol Psychiatry 48:971–975.

SUPPLEMENTARY INFORMATION

Individualized Functional Brain System Topologies and Major Depression: Relations Among Patch Sizes and Clinical Profiles and Behavior

Sacchet *et al.*

This PDF file includes:

Supplementary Participant Information

Most participants in this study provided all clinical/behavioral data with no missing variables (see **Tables S1** and **S2**). Recruitment spanned four institutions (Columbia University, Massachusetts General Hospital, University of Michigan, and UT Southwestern) that participated in a multi-site clinical trial – the Establishing Moderators and Biosignatures of Antidepressant Response for Clinical Care for Depression (EMBARC)[1]. For the current study, analyses were conducted solely on data from the baseline assessment prior to pharmacological intervention. The Structured Clinical Interview for DSM-IV[2] was used to determine if participants met diagnostic criteria for MDD currently in episode. Additional inclusion criteria for MDD participants included presence of depression symptoms above an established cut-off score (≥14) on the Quick Inventory of Depression Symptomatology[1]. Participants identified as American Indian/Alaska Native (0.3%), Asian (7%) Black or African American (20%), more than one race (8%), and White (65%).

Supplementary Methods

Measures

Clinical Assessments

Quick Inventory of Depressive Symptomatology-Self Report (QIDS-SR). The QIDS-SR is a 16-item self-report scale for depressive symptom severity. The QIDS-SR has been shown to have high internal consistency and to be a valid and sensitive measure of depressive symptom change in clinical research settings[3].

Hamilton Rating Scale for Depression (HRSD). The HRSD is a clinician-administered measure of depression severity[4], and is widely used in clinical trial research.

Snaith-Hamilton pleasure scale (SHAPS). The SHAPS is a 14-item validated measure of anhedonia[5,6]. Anhedonia is a key endophenotype of depression related to dysfunctional reward-processing and therefore assessed alongside reward-task behavior[7,8].

Mood and Anxiety Symptom Questionnaire (MASQ). The MASQ is a 30-item self-report symptom scale with three subscales of clinical interest: anxious arousal, general distress, and anhedonia[9].

Behavioral Tasks

The Probabilistic Reward Task (PRT). Rooted in signal detection theory, the PRT uses an asymmetrical reinforcement schedule to assess reward learning (i.e., the ability to modulate behavior as a function of rewards)[8]. In each trial, participants must decide which between two difficult-to-discriminate stimuli has been briefly presented (100 ms). Unbeknownst to participants, correct identifications of one stimulus are rewarded three times more frequently than the other, eliciting a response bias (RB; i.e., preference for the more frequently rewarded stimulus), which has been shown to be lower in MDD, specifically among anhedonic individuals[7,8,10]. Reward learning was operationalized as the increase in response bias between the two blocks administered within the EMBARC study (i.e., ΔRB = RB[Block 2] – RB[Block 1]). Data from 255 MDD participants who passed the quality control were included in the PRT analyses**.** Criteria for quality controls were based on a prior EMBARC paper[11] and are described below.

PRT Quality Controls. Participants were excluded if they had less than 80 valid trails in each block; less than 24 rich rewards or less than 7 lean rewards in each block; rich-to-lean reward ratio less than 2.5 in any block; or rich or lean accuracy less than 0.40 in any block. Valid trails were defined as trails with less than 20% outlier responses, which were responses where reaction time was shorter than 150 ms or greater than 2,500 ms and the log-transformed reaction time exceeded the participant's mean by 3 standard deviations.

Flanker Task. The Flanker Task assesses response conflict and error monitoring/adjustments[12,13]. Flanker Task data from 257 MDD participants passed quality control and were included in subsequent analyses. Criteria for quality controls were based on a prior EMBARC paper[11] and can be found below. In each trial, participants are shown five arrows and indicate whether the

center arrow points to the left or right. On 66% of trials, the direction of the center arrow is congruent with the flanking arrows, while incongruent on remaining trials. Primary variables include interference effects on reaction time ($RT_{Incongurent} - RT_{Congurent}$;) and accuracy ($Accuracy_{Congurent} - Accuracy_{Incongurent}$;), with higher values reflecting increased interference (i.e., worse cognitive control).

Flanker Quality Controls. Participants were excluded if they had greater than 35 RT outlier trials, less than 200 non-outlier congruent trials, fewer than 90 non-outlier incongruent trials, or less than 50% correct for congruent or incongruent trials. Outlier trials were defined as trials in which the reaction time was less than 150 ms or log-transformed reaction time exceeded the participant's mean by 3 standard deviations (calculated separately for congruent and incongruent stimuli).

A-not-B task. The A-not-B task assesses working memory and reasoning, and has been related to antidepressant response[14,15]. Participants read a statement during each trial describing a two-letter arrangement order and were asked to rapidly evaluate the statement as true or false. (e.g., Statement: "A comes before B", presented below statement: "BA", correct participant response: False). Primary variables used were number of and RTs for correct responses.

MRI Acquisition and Preprocessing

Structural and functional MRI data were collected at each site using 3T MRI scanners. MRI data from EMBARC (emotional conflict task[16], reward processing task[17,18] and two resting-state runs) were included in the present study. 318 subjects out of 328 subjects had all four MRI runs (see **Table S2** for details). Preprocessing was performed using FreeSurfer[19] with fMRIPrep 20.0.5[20,21].

Acquisition Parameters. Columbia University scanned with a General Electric Discovery MR750 3T system with the following parameters – Structural scan: FSPGR, TR=6.0ms, TE=2.4ms, TI=900 ms, Flip Angle = 9°, FOV=256×256 mm, Slice Thickness=1 mm, Matrix=256×256, 178 total slices. Functional scan: TR/TE=2000/28ms, Flip Angle**=**90°, FOV=205×205 mm, Slice thickness=3.1mm, Matrix=64×64.

At Massachusetts General Hospital, a Siemens Trio 3T system was used with the following parameters – Structural scan: MPRAGE, TR=2300ms, TE=2.54 ms, TI=900ms, Flip Angle=9°, FOV=256×256mm, Slice Thickness=1 mm, Matrix=256×256, 176 total slices. Functional scan: TR/TE=2000/28ms, Flip Angle**=**90°, FOV=205×205mm, Slice thickness=3.1mm, Matrix=64×64.

At University of Michigan, a Phillips Ingenia 3T system was used. Structural scan: Turbo Field Echo (TFE), TR=8.2ms, TE=3.7ms, TI=1100ms, Flip Angle=12°, FOV=256×256mm, Slice Thickness=1mm,
Matrix=256×256, 178 continuous slices. Functional scan: TR/TE=2000/28ms, Flip Angle=90°, FOV=205×205mm, Slice thickness=3.1mm, Matrix=64×64.

Finally, the University of Texas Southwestern Medical Center used a Phillips Achieva 3T scanner. Structural scan: MPRAGE, TR=2100ms, TE=3.7ms, TI=1100ms, Flip Angle=12°, FOV=256×256mm, Slice Thickness=1mm, Matrix=256×256, 178 continuous slices. Functional scan: TR/TE=2000/28ms, Flip Angle=90°, FOV=205×205mm, Slice thickness=3.1mm, Matrix=64×64.

Run time and total volumes for MRI runs can be found in Table S4. Pre-processing included discarding 4 initial volumes, bandpass filtering (0.009-0.08 Hz), nuisance signal regression (white matter, cerebrospinal fluid, and 12 head-motion parameters), projecting data to a common fsaverage6 spherical coordinate system, smoothing with a 6-mm Gaussian kernel, and down-sampling to a standard fsaverage4 surface mesh (2,562 vertices per hemisphere). The resulting surface space data were further processed using the individualized brain mapping procedure.

Subject-wise framewise displacement (FD) and percent signal change between volumes (DVARS) were calculated via a weighted average of task-specific means averages by runtime across sites.

Scan Duration

Scan duration of the study can be found in Table S4. Individualized system mapping, including the methods proposed, have been shown to exhibit high reproducibility and reliability with as little as 12 or 8 min of fMRI data[22–24]. Since the EMBARC data constitutes a total of 33 minutes of scan time, the

proposed datasets have more than sufficient data for reliable individualized system mapping (>20 min). Further, prior studies utilizing the same methodologies described here, were able to establish reliability of system assignment with a total scan duration of less than 30 minutes per subject[24–26].

Mapping Cortical Individualized Brain Systems

Our primary individualized systems mapping approach is based on an iterative optimization method[24,26–28]. For each participant, a system atlas (Yeo Atlas) was systematically and iteratively remapped to incorporate more person-specific information. This culminates in convergence on a person-specific map (i.e., individualized brain systems). The procedure includes several steps. First a 17-brain system atlas based on 1,000 fMRI datasets is used for initialization of the iterative optimization procedure, timecourses are then averaged across vertices in each system, and the use of these signals for reference of individualized optimization. Then, the signal at each vertex was correlated to each of the 17 reference signals, and the vertex was assigned to the system with which it exhibits the greatest correlation. Nearby vertices were not omitted when extracting the reference signals. To explore the bias of nearby vertices, the similarity of individualized networks when using the original group-average atlas and atlas omitted nearby vertices were tested. The individualized networks were reliable (Dice's coefficient = 0.91) by omitting nearby vertices of group-average priors. Confidence values were computed as the ratio between the largest and next-largest correlation. Next, core signals were computed for each system as the mean timecourse across vertices with confidence values >1.1. Parameters were computed for each system: inter-subject variability in correlations and temporal signal-to-noise ratio (SNR). For each system, reference and core signals were averaged using weighting that incorporated inter-individual variability, SNR, and current iteration number. The resulting signal was used as a new reference signal as in prior steps iteratively. Weighting ensured that the influence of the atlas-based reference signal was reduced in regions of high inter-subject variability and SNR. These steps were repeated until 99% of vertices remained in the same system as the prior iteration (i.e., convergence). For each individual, this resulted in mapping of individualized brain systems.

Supplementary Tables and Figures

Supplementary Table 1. Sample Sizes for Clinical and Behavioral Variables. Data included for clinical and behavioral measures.

Behavioral Measure	MDD
	N
Mood and Anxiety Symptom Questionnaire	
Anxious Arousal	287
Anhedonia	287
General Distress	287
Hamilton Rating Scale for Depression	288
Snaith-Hamilton Pleasure Scale	288
Quick Inventory of Depressive Symptomatology – Self Report	288
Probabilistic Reward Task *	255
Flanker (ms)*	
Reaction Time	257
Accuracy	257
A-not-B Task	
Reaction Time (ms)	285
Total correct responses (%)	285

MDD=Major Depressive Disorder.

*Additional quality control criteria were used on all available data. *N* represents subjects who passed quality control criteria.

Supplementary Table 2. Participant MRI Data Availability. This table indicates available fMRI data for each task type. The available fMRI data included an emotion recognition task (ERT), resting state (runs 1 and 2), and the reward processing task.

MRI runs	
	N
Healthy Control Group	
emotion recognition task, resting state 1	0
emotion recognition task, resting state 1, resting state 2	1
emotion recognition task, resting state 1, resting state 2, reward*	39
emotion recognition task, resting state 1, reward	0
resting state 1	0
resting state 1, resting state 2	0
resting state 1, resting state 2, reward	0
Total Participants	**40**
Major Depressive Disorder Group	
emotion recognition task, resting state 1	2
emotion recognition task, resting state 1, resting state 2	1
emotion recognition task, resting state 1, resting state 2, reward*	279
emotion recognition task, resting state 1, reward	1
resting state 1	2
resting state 1, resting state 2	2
resting state 1, resting state 2, reward	1
Total Participants	**288**

N=Number of Subjects; *participants for which all four fMRI runs were available.

Supplementary Table 3: Neurosynth Quantitative De-coding. Neurosynth was used to meta-analytically decode patch vertices of the lateral salience brain system parietal operculum and control brain system left medial posterior prefrontal cortex. This analysis resulted in meta-analytic key words related to the target regions. The highest and lowest 20 key words are arranged by correlation strength. Each key term is provided with a correlation value in the accompanying column.

Lateral salience system parietal operculum: Neurosynth Findings				**Left control system medial posterior prefrontal cortex: Neurosynth Findings**			
Highest Correlations (r)		**Lowest Correlations (r)**		**Highest Correlations (r)**		**Lowest Correlations (r)**	
tactile	0.316	autobiographical	-0.024	domain general	0.127	movements	-0.006
supramarginal gyrus	0.308	medial	-0.024	chinese	0.119	motor	-0.006
supramarginal	0.300	vi	-0.023	ventral dorsal	0.118	cerebellum	-0.006
somatosensory cortex	0.291	memory	-0.021	ventrolateral	0.109	vi	-0.005
secondary somatosensory	0.288	faces	-0.021	dorsomedial	0.108	pain	-0.005
somatosensory	0.285	episodic	-0.020	judgement	0.092	autobiographical	-0.005
stimulation	0.273	task	-0.020	reasoning	0.091	sensorimotor	-0.005
pain	0.257	occipital	-0.019	pfc	0.086	primary motor	-0.005
touch	0.257	intraparietal	-0.019	medial frontal	0.079	motor cortex	-0.005
somatosensory cortices	0.255	orbitofrontal	-0.019	pre supplementary	0.070	cerebellar	-0.005
s1	0.239	medial prefrontal	-0.019	motor pre	0.068	motor imagery	-0.005
painful	0.239	vermis	-0.019	retention	0.062	execution	-0.005
primary somatosensory	0.211	semantic	-0.019	anterior prefrontal	0.058	finger	-0.005
sii	0.211	reward	-0.019	pairs	0.053	temporal	-0.005
ipsilateral	0.175	reading	-0.018	cortex pfc	0.051	visual	-0.005
electrical	0.170	language	-0.018	success	0.050	hand	-0.005
noxious	0.150	words	-0.018	semantic	0.050	premotor cortex	-0.005
sensory	0.149	tasks	-0.018	recognition memory	0.050	somatosensory	-0.005
contralateral	0.146	orbitofrontal cortex	-0.018	pre sma	0.490	lobules	-0.005
imagine	0.137	nuclei	-0.018	ventrolateral prefrontal	0.047	movement	-0.005

Supplementary Table 4: Run time and total volumes for MRI data. This table shows the total time taken and total volume for each MRI run.

MRI Runs	Total Time	Total Volume
rest 1	6 minutes	180
rest 2	6 minutes	180
emotion recognition task	13 minutes	397
reward	8 minutes	240

Supplementary Table 5: Relations among Individualized Brain Systems Patch Sizes and Behavioral Variables using Pearson correlation. This table includes correlation results between individualized brain system patches and hypothesized behavioral correlations performed using Pearson correlations regardless of normality.

Medial posterior prefrontal cortex		
Behavioral Measure	**Pearson Correlation**	
	rho	**pval**
Flanker Accuracy	0.057	0.361
Flanker Reaction Time	0.012	0.846
PRT reward learning	0.054	0.394
Snaith-Hamilton pleasure scale	-0.094	0.112
MASQ – Anxious Arousal	0.032	0.590
MASQ – Anhedonia	-0.087	0.140
MASQ – General Distress	-0.035	0.553
Hamilton Rating Scale for Depression	0.032	0.585
QIDS - SR	-0.055	0.356
A not B – Reaction time	0.021	0.727
A not B – Total correct	-0.121	0.041*
Lateral Salience System		
Behavioral Measure	**Pearson Correlation**	
	rho	**pval**
Flanker Accuracy	0.075	0.233
Flanker Reaction Time	-0.117	0.061
PRT reward learning	-0.135	0.031*
Snaith-Hamilton pleasure scale	-0.044	0.458
MASQ – Anxious Arousal	-0.121	0.040*
MASQ – Anhedonia	-0.111	0.059
MASQ – General Distress	-0.081	0.169
Hamilton Rating Scale for Depression	-0.101	0.087
QIDS - SR	-0.079	0.182
A not B – Reaction time	-0.050	0.403
A not B – Total correct	-0.046	0.436

Supplementary Table 6: Surface Area Differences in Significant Individualized Brain System Patch Sizes by Group. This table shows differences in surface area of the medial posterior prefrontal cortex and parietal operculum, which were previously found to be significantly smaller in MDD subjects compared to controls based on patch size measured by number of vertices. Statistical significance indicated: $^{*}p < 0.05$. $^{**}p < 0.01$. $^{***}p < 0.001$.

Region	**MDD**		**HC**			
	M/Mdn	***SD/IQR***	***M/Mdn***	***SD/IQR***	***p*-value**	**test statistic**
L medial posterior prefrontal cortex B (control system)	-0.604	3.390	0.893	3.270	0.000***	-3.501
Parietal Operculum (lateral salience system)	-1.501	17.241	6.294	19.638	0.005**	-2.834

Data represent surface area. Data were non-normally distributed and Wilcoxon rank-sum tests were used for statistical assessment with medians (Mdn) and interquartile ranges (IQR) reported. L=left hemisphere; R=right hemisphere, HC = Healthy Controls. Statistical significance indicated: $^{*}p < 0.05$. $^{**}p < 0.01$. $^{***}p < 0.001$.

Supplementary Table 7: Differences in Significant Individualized Brain System Patch Sizes by Group. This table shows differences in individualized system patch sizes based on raw values of patch size estimation (i.e, without regressing nuisance variables).

Region	MDD		HC			
	M/Mdn	*SD/IQR*	*M/Mdn*	*SD/IQR*	*p*-value	test statistic
Lateral Salience System						
Insula A[2]	92	21	91.5	16	0.756	-0.311
Insula B[2]	87	18	86	17.5	0.982	0.023
Frontal operculum[2]	58	17.5	57	14.5	0.842	-0.199
Parietal operculum[1]	77.5	21.5	90.4	19.8	0.000***	-3.58
Inferior parietal lobule[1]	20.5	10.3	23.3	8.6	0.107	-1.619
Medial Salience System						
Medial posterior prefrontal cortex[2]	72	24	70.5	15.5	0.083	1.736
Frontal medial[2]	79	19.5	82	17	0.167	-1.382
Parietal medial[1]	52.1	17.2	57.2	14.6	0.072	-1.804
Control System						
L dorsal prefrontal cortex A[2]	11	9	10	8.5	0.51	0.659
L dorsal prefrontal cortex B [2]	7	13	6.5	11	0.707	0.375
L lateral prefrontal cortex B [2]	22	10	22	8	0.488	-0.694
L medial posterior prefrontal cortex B[2]	5	5	8	4.5	0.001**	-3.32
R medial posterior prefrontal cortex B[2]	12	8	14	9	0.109	-1.604
R lateral prefrontal cortex A[2]	50	17.5	50.5	12	0.402	-0.838
L lateral ventral prefrontal cortex A[2]	15	7	17	5	0.012	-2.502
R lateral dorsal prefrontal cortex B[1]	43.1	11.7	43.9	9.7	0.651	-0.453
R dorsal prefrontal cortex A[2]	13	12	15	10.5	0.465	-0.731
L lateral prefrontal cortex A[1]	41.7	9.5	42.2	7.1	0.742	-0.329
L lateral ventral prefrontal cortex B[2]	32	13	34.5	8	0.069	-1.821
R lateral ventral prefrontal cortex B[2]	43	14	47.5	13.5	0.134	-1.5
Default System						
Precuneus posterior cingulate cortex[2]	97	17	97.5	16.5	0.725	-0.352
Retrosplenial[2]	56	14	54	18.5	0.197	1.289
Medial prefrontal cortex[2]	103	34.5	105.5	25	0.183	-1.331
Affective System						
Orbital frontal cortex[1]	174.4	35.9	168.9	32.8	0.364	0.91
Temporal pole[2]	172.5	59	159	63	0.186	1.323

Data represent raw values. [1]Data were normally distributed and *t*-tests were used for statistical assessment with means (M) and standard deviations (SD) reported. [2]Data were non-normally distributed and Wilcoxon rank-sum tests were used for statistical assessment with medians (Mdn) and interquartile ranges (IQR) reported. L=left hemisphere; R=right hemisphere, HC = Healthy Controls. Statistical significance indicated following FDR correction: $^{*}p < 0.05$. $^{**}p < 0.01$. $^{***}p < 0.001$.

Supplementary Table 8: Exploratory Analyses of Patch Size Differences by Group in Attention and Somatomotor Systems.

Region	MDD		HC			
	M/Mdn	*SD/IQR*	*M/Mdn*	*SD/IQR*	*p*-value	test statistic
Dorsal Attention System						
Temporal occipital A[1]	-0.68	22.41	4.89	22.41	0.143	-1.468
Parietal occipital[1]	0.36	17.07	-2.56	17.07	0.315	1.007
Superior parietal lobule[2]	-0.89	29.28	-3.5	29.95	0.348	0.939
Temporal occipital B[2]	-1.29	8.78	-2.11	8.91	0.211	1.250
Post central[2]	-0.75	35.9	0.02	27.68	0.893	0.134
Frontal eye fields[2]	-1.09	19.69	-2.16	15.47	0.836	-0.207
Precentral ventral[2]	-1.45	11.07	-2.41	9.71	0.721	0.357
Somatomotor System						
Somatomotor A[2]	2.35	35.29	3.74	34.23	0.999	0.001
Central[2]	1.18	17.65	3.37	21.67	0.646	-0.460
S2[2]	2.93	21.04	-2.97	20.27	0.165	1.389
Insula[2]	-0.14	10.21	-2.31	8.52	0.202	1.275
Auditory[2]	3.17	17.61	-0.5	14.53	0.091	1.690
Salience/Ventral Attention System						
Parietal operculum[1]	-1.28	20.17	9.25	19.49	0.002**	-3.106
Parietal medial[1]	-0.27	15.23	1.92	14.13	0.392	-0.857
Insula A[2]	-0.5	18.41	0.02	16.09	0.827	0.218
Frontal operculum[2]	-1.36	15.85	-0.65	13.56	0.642	0.465
Frontal medial[2]	-0.63	18.82	2.21	15.25	0.342	-0.949
R precentral[2]	-0.56	7.53	-1.75	8	0.339	0.956
Insula B[2]	-0.37	18.16	0.66	14.1	0.465	-0.730
Inferior parietal lobule[2]	-0.41	11.59	-0.95	11.77	0.656	-0.446
Dorsal prefrontal cortex	-0.82	7.82	-0.12	8.3	0.348	0.939
Lateral prefrontal cortex[2]	-0.33	20.04	-2.94	18.38	0.373	0.891
L orbital frontal cortex[2]	-0.7	1.17	-0.64	2.82	0.583	-0.549
Medial posterior prefrontal cortex[2]	-1.31	21.91	-1.52	13.97	0.952	0.060
R lateral ventral prefrontal cortex[2]	0.43	12.64	1.44	10.84	0.390	-0.860

Data are residuals. [1]Data were normally distributed and *t*-tests were used for statistical assessment with means (M) and standard deviations (SD) reported. [2]Data were non-normally distributed and Wilcoxon rank-sum tests were used for statistical assessment with medians (Mdn) and interquartile ranges (IQR) reported. L=left hemisphere; R=right hemisphere, HC = Healthy Controls. Statistical significance indicated: $^{*}p < 0.05$. $^{**}p < 0.01$. $^{***}p < 0.001$.

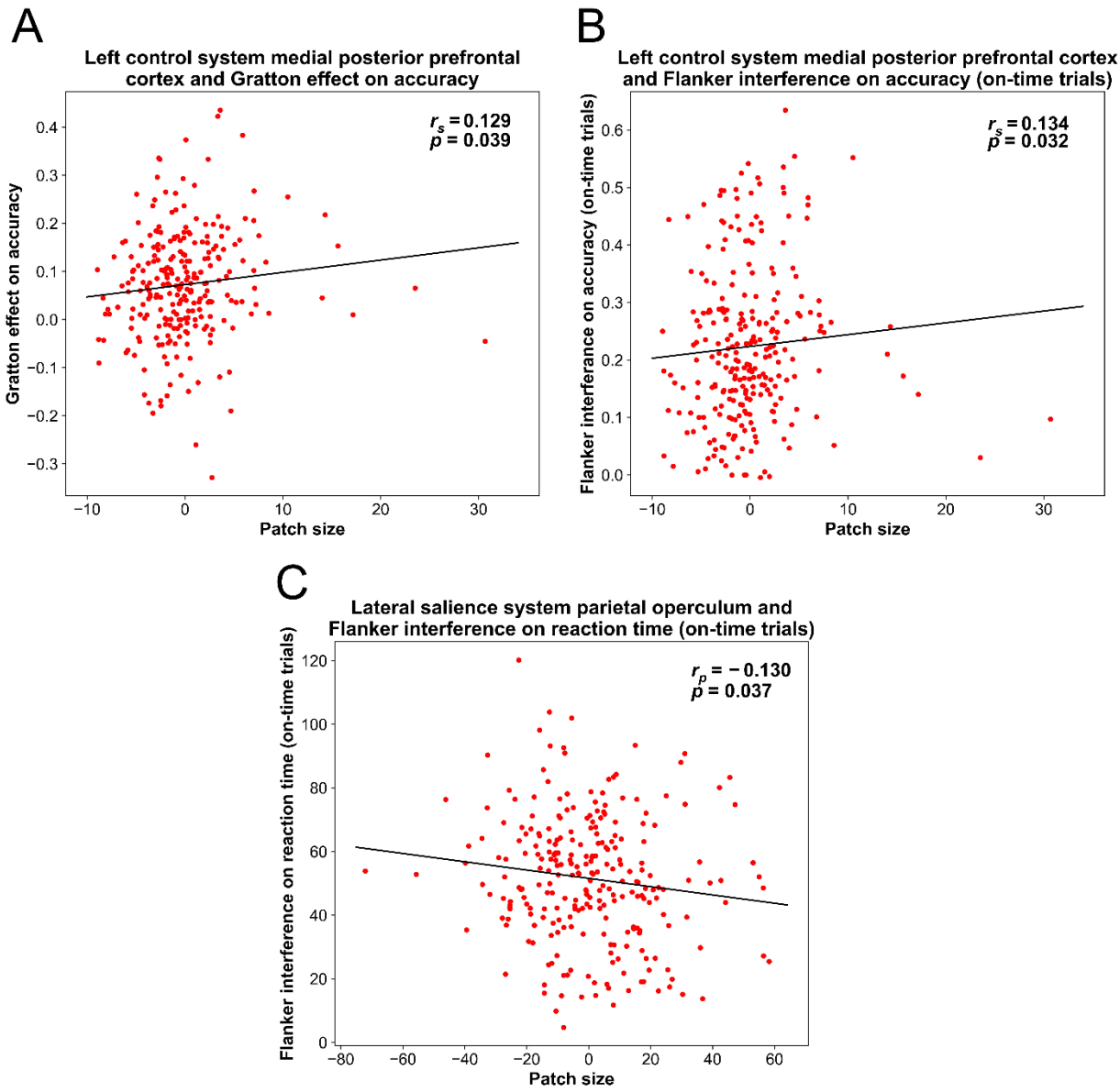

Supplementary Figure 1. Relations among Individualized Brain Systems Patch Sizes and Additional Flanker Task Variables. Panels A and B: Correlations between medial posterior prefrontal cortex control system patch size (residualized number of vertices) and behavioral measures of (A) Flanker task: Gratton effect on accuracy that measures the effects of trial history; such that higher values indicate increased stimulus-induced conflict and (B) Flanker interference effects on accuracy for on-time trials. Panel C: Correlations between parietal operculum salience system patch size and Flanker task reaction time for on-time trials. r_p=Pearson correlation coefficient; p=p-value; r_s= Spearman correlation coefficient. Note: None of the flanker exploratory measures survived FDR correction.

Supplementary References

1. Trivedi MH, McGrath PJ, Fava M, et al. Establishing moderators and biosignatures of antidepressant response in clinical care (EMBARC): Rationale and design. *J Psychiatr Res*. 2016;78:11-23. doi:10.1016/j.jpsychires.2016.03.001

2. First MB, Spitzer RL, Gibbon M, Williams JBW. *Structured Clinical Interview for DSM-IV-TR Axis I Disorders, Research Version, Patient Edition (SCID-I/P)*. New York: Biometrics Research, New York State Psychiatric Institute.; 2002a.

3. Rush AJ, Trivedi MH, Ibrahim HM, et al. The 16-Item Quick Inventory of Depressive Symptomatology (QIDS), clinician rating (QIDS-C), and self-report (QIDS-SR): a psychometric evaluation in patients with chronic major depression. *Biol Psychiatry*. 2003;54(5):573-583. doi:10.1016/s0006-3223(02)01866-8

4. Hamilton M. A rating scale for depression. *J Neurol Neurosurg Psychiatry*. 1960;23:56-62. doi:10.1136/jnnp.23.1.56

5. Snaith RP, Hamilton M, Morley S, Humayan A, Hargreaves D, Trigwell P. A scale for the assessment of hedonic tone the Snaith-Hamilton Pleasure Scale. *Br J Psychiatry J Ment Sci*. 1995;167(1):99-103. doi:10.1192/bjp.167.1.99

6. Franken IHA, Rassin E, Muris P. The assessment of anhedonia in clinical and non-clinical populations: further validation of the Snaith-Hamilton Pleasure Scale (SHAPS). *J Affect Disord*. 2007;99(1-3):83-89. doi:10.1016/j.jad.2006.08.020

7. Pizzagalli DA, Jahn AL, O'Shea JP. Toward an objective characterization of an anhedonic phenotype: a signal-detection approach. *Biol Psychiatry*. 2005;57(4):319-327. doi:10.1016/j.biopsych.2004.11.026

8. Pizzagalli DA, Iosifescu D, Hallett LA, Ratner KG, Fava M. Reduced Hedonic Capacity in Major Depressive Disorder: Evidence from a Probabilistic Reward Task. *J Psychiatr Res*. 2008;43(1):76-87. doi:10.1016/j.jpsychires.2008.03.001

9. Watson D, Clark LA, Weber K, Assenheimer JS, Strauss ME, McCormick RA. Testing a tripartite model: II. Exploring the symptom structure of anxiety and depression in student, adult, and patient samples. *J Abnorm Psychol*. 1995;104(1):15-25. doi:10.1037//0021-843x.104.1.15

10. Vrieze E, Pizzagalli DA, Demyttenaere K, et al. Reduced reward learning predicts outcome in major depressive disorder. *Biol Psychiatry*. 2013;73(7):639-645. doi:10.1016/j.biopsych.2012.10.014

11. Webb CA, Dillon DG, Pechtel P, et al. Neural Correlates of Three Promising Endophenotypes of Depression: Evidence from the EMBARC Study. *Neuropsychopharmacology*. 2016;41(2):454-463. doi:10.1038/npp.2015.165

12. Holmes AJ, Bogdan R, Pizzagalli DA. Serotonin Transporter Genotype and Action Monitoring Dysfunction: A Possible Substrate Underlying Increased Vulnerability to Depression. *Neuropsychopharmacology*. 2010;35(5):1186-1197. doi:10.1038/npp.2009.223

13. Eriksen BA, Eriksen CW. Effects of noise letters upon the identification of a target letter in a nonsearch task. *Percept Psychophys*. 1974;16(1):143-149. doi:10.3758/BF03203267

14. Baddeley AD. A 3 min reasoning test based on grammatical transformation. *Psychon Sci*. 1968;10(10):341-342. doi:10.3758/BF03331551

15. Gorlyn M, Keilp JG, Grunebaum MF, et al. Neuropsychological characteristics as predictors of SSRI treatment response in depressed subjects. *J Neural Transm Vienna Austria 1996*. 2008;115(8):1213-1219. doi:10.1007/s00702-008-0084-x

16. Etkin A, Egner T, Peraza DM, Kandel ER, Hirsch J. Resolving Emotional Conflict: A Role for the Rostral Anterior Cingulate Cortex in Modulating Activity in the Amygdala. *Neuron*. 2006;51(6):871-882. doi:10.1016/j.neuron.2006.07.029

17. Forbes EE, Olino TM, Ryan ND, et al. Reward-Related Brain Function as a Predictor of Treatment Response in Adolescents with Major Depressive Disorder. *Cogn Affect Behav Neurosci*. 2010;10(1):107-118. doi:10.3758/CABN.10.1.107

18. Forbes EE, Ryan ND, Phillips ML, et al. Healthy Adolescents' Neural Response to Reward: Associations with Puberty, Positive Affect, and Depressive Symptoms. *J Am Acad Child Adolesc Psychiatry*. 2010;49(2):162-172e5.

19. Fischl B. FreeSurfer. *NeuroImage*. 2012;62(2):774-781. doi:10.1016/j.neuroimage.2012.01.021

20. Esteban O, Markiewicz CJ, Blair RW, et al. fMRIPrep: a robust preprocessing pipeline for functional MRI. *Nat Methods*. 2019;16(1):111-116. doi:10.1038/s41592-018-0235-4

21. Gorgolewski K, Burns C, Madison C, et al. Nipype: A Flexible, Lightweight and Extensible Neuroimaging Data Processing Framework in Python. *Front Neuroinformatics*. 2011;5. Accessed April 12, 2022. https://www.frontiersin.org/article/10.3389/fninf.2011.00013

22. Gordon EM, Laumann TO, Adeyemo B, et al. Individual-specific features of brain systems identified with resting state functional correlations. *NeuroImage*. 2017;146:918-939.

23. Kong R, Li J, Orban C, et al. Spatial Topography of Individual-Specific Cortical Networks Predicts Human Cognition, Personality, and Emotion. *Cereb Cortex*. 2019;29:2533-2551.

24. Wang D, Buckner RL, Fox MD, et al. Parcellating cortical functional networks in individuals. *Nat Neurosci*. 2015;18(12):1853-1860. doi:10.1038/nn.4164

25. Brennan BP, Wang D, Li M, et al. Use of an Individual-Level Approach to Identify Cortical Connectivity Biomarkers in Obsessive-Compulsive Disorder. *Biol Psychiatry Cogn Neurosci Neuroimaging*. 2019;4(1):27-38. doi:10.1016/j.bpsc.2018.07.014

26. Wang D, Li M, Wang M, et al. Individual-specific functional connectivity markers track dimensional and categorical features of psychotic illness. *Mol Psychiatry*. 2020;25(9):2119-2129. doi:10.1038/s41380-018-0276-1

27. Li M, Wang D, Ren J, et al. Performing group-level functional image analyses based on homologous functional regions mapped in individuals. Rushworth M, ed. *PLOS Biol*. 2019;17(3):e2007032. doi:10.1371/journal.pbio.2007032

28. Brennan BP, Wang D, Li M, et al. Use of an Individual-Level Approach to Identify Cortical Connectivity Biomarkers in Obsessive-Compulsive Disorder. *Biol Psychiatry Cogn Neurosci Neuroimaging*. 2019;4(1):27-38. doi:10.1016/j.bpsc.2018.07.014